Determination of homogeneous and inhomogeneous broadening in semiconductor nanostructures by two-dimensional Fourier-transform optical spectroscopy

I. Kuznetsova,[1] T. Meier,[1,2] S. T. Cundiff,[3] and P. Thomas[1]
[1]*Department of Physics and Material Sciences Center, Philipps University, Renthof 5, D-35032 Marburg, Germany*
[2]*Department Physik, Fakultät für Naturwissenschaften, Universität Paderborn, Warburger Strasse 100, D-33098 Paderborn, Germany*
[3]*JILA, University of Colorado and National Institute of Standards and Technology, Boulder, Colorado 80309-0440, USA*
(Received 12 April 2007; revised manuscript received 28 June 2007; published 2 October 2007)

The imaginary part of two-dimensional Fourier-transform spectra in the rephasing and nonrephasing modes is used to analyze the homogeneous and inhomogeneous broadening of excitonic resonances in semiconductor nanostructures. Microscopic calculations that include heavy- and light-hole excitons as well as coherent biexcitonic many-body correlations reveal distinct differences between the rephasing and nonrephasing spectra. A procedure is proposed that allows separation of disorder-induced broadening in complex systems that show several coupled resonances.

DOI: 10.1103/PhysRevB.76.153301 PACS number(s): 78.47.+p, 42.50.Md, 42.65.Re, 78.67.−n

In the past decades, various optical techniques have been used to investigate and unravel the structure of electronic states in semiconductor nanostructures and other material systems.[1–5] Spatially resolved linear optical measurements give information about homogeneous and inhomogeneous broadening separately. Typically, however, they provide only general information, e.g., the total linewidth. On the other hand, nonlinear experiments have been applied successfully to obtain much more detailed information about the nature of excited states, the coupling among them, and many-body effects. In addition, different nonlinear optical techniques were used to investigate the amounts of homogeneous and inhomogeneous broadening (see Ref. 5 and references therein).

Pump-probe measurements provide one-dimensional spectral information that cannot distinguish between homogeneous and inhomogeneous broadening. Hole burning can find the homogeneous contribution to the optical linewidth and, by comparing to the linear spectrum, provides an estimate of the inhomogeneous contribution. Four-wave-mixing (FWM) experiments show photon echoes in the time-resolved (TR) traces.[5,6] Their temporal width is determined by the inhomogeneous linewidth. However, for systems where more than a single resonance is simultaneously excited, the width of the echo is ill defined due to beating,[5,7,8] in particular, for small inhomogeneous broadening see (Fig. 1). The time-integrated (TI) trace yields the homogeneous width, i.e., the dephasing rate. However, in the presence of more than just a single optical resonance, the decay parameter cannot uniquely be determined and a fitting procedure is needed.

In semiconductor nanostructures, many-body Coulomb interaction strongly alters the nonlinear optical response.[3–5,9,10] Even at the Hartree-Fock level, e.g., the line shape of time-resolved FWM is significantly modified and signals for the *wrong* time ordering appear.[3–5,11,12] Additionally, already in the low-intensity third-order $[\chi^{(3)}]$ limit, characteristic dependencies of the nonlinear transients and spectra on the polarization directions of the incident pulses and couplings among optically isolated resonances appear due to many-body correlations.[3–5,9,13–17]

A detailed microscopic description of interacting excitons in the presence of disorder is a formidable task. Thus, well-established knowledge is lacking on this topic. It was, however, shown that Hartree-Fock renormalizations influence the temporal width of photon echoes in weakly disordered semiconductor quantum wells.[18] Very interesting biexciton-induced polarization-dependent quantum beats have been measured in strongly disordered quantum wells and were modeled on the basis of a simplified level scheme in Ref. 19. Later, it became possible to describe these phenomena on the basis of a microscopic many-body theory that phenomenologically includes disorder-induced inhomogeneous broadening.[20] Reference 21 includes both biexciton correlations and disorder on a microscopic level. The numerically computed FWM transients presented there show, in agreement with experiments, a polarization-dependent disorder-induced dephasing, i.e., a disorder-induced decay of the

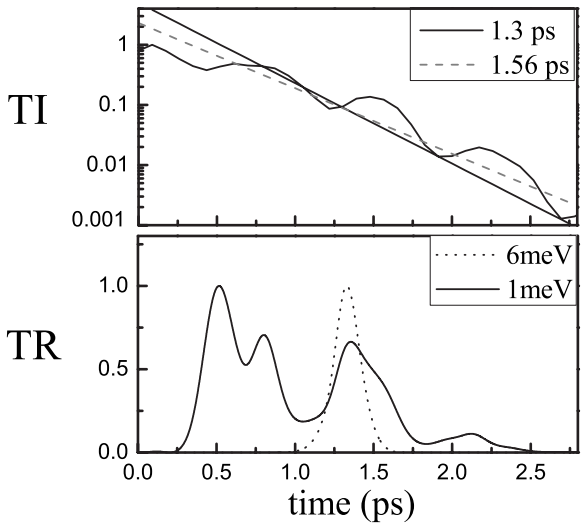

FIG. 1. Time-integrated and time-resolved traces for $\sigma^+\sigma^+\sigma^+$ excitation. The TI (TR) data have been calculated using inhomogeneous Gaussian broadening $\gamma^{inhom}=1$ meV ($\gamma^{inhom}=1$ and 6 meV). Dipole matrix elements are taken to be identical, $T_2^{h,l}=1.3$ ps. Straight lines correspond to dephasing times 1.3 and 1.56 ps, respectively.

FWM amplitude that depends on the polarization directions of the incident beams.

Recently, two-dimensional Fourier-transform spectroscopy (2D-FTS) has been applied to investigate the excitonic response of semiconductor quantum wells.[22–27] This method enables the simultaneous measurement of the phase and the amplitude for various polarization directions of the excitation pulses. 2D-FTS is based on concepts developed in magnetic resonance.[28] Recently, infrared and visible implementations of 2D-FTS have been used to study vibrational[29,30] and electronic excitations[31–33] in molecules. For the analysis of excitons in semiconductor quantum wells, 2D coherent-excitation spectroscopy (CES) has been used.[17,34,35] This measurement is based on partially nondegenerate FWM[36] using a temporally long pulse and a short pulse, i.e., a spectrally narrow pulse and a broad pulse. Therefore, it provides mainly spectral and little temporal information. Furthermore, CES has only been used to measure intensities, i.e., it lacks the phase information provided by 2D-FTS.

In this work, we suggest, on the basis of the aforementioned microscopic model calculations, that 2D-FTS can be used for the detailed study of homogeneous and inhomogeneous broadening of optical resonances. It is demonstrated that with this technique, it is possible to extract information on the disorder-induced broadening, separately for each resonance of a complex coupled system.

The optical pulses are denoted by a, b, c, and s, where a, b, and c refer to the incident beams and s to the nonlinear signal. If $\mathbf{k}_i$ denotes the propagation direction of pulse i, the signal is monitored in the direction $\mathbf{k}_s=\mathbf{k}_b+\mathbf{k}_c-\mathbf{k}_a$. A detailed discussion of the experimental box-configuration setup can be found in Ref. 22. Depending on the temporal order of the pulses a and b, one denotes the experimental mode by rephasing (a preceding b) and nonrephasing (b preceding a), respectively. When the signal is time resolved, the rephasing configuration yields photon echoes if the sample is characterized by an inhomogeneous line, whereas the echoes are absent for the wrong time ordering,[1–5,11] i.e., the nonrephasing mode. (We note that the nonrephasing configuration does not correspond to negative delay in a two pulse experiment, which would be equivalent to a arriving after both b and c, whereas in the nonrephasing configuration c arrives last.)

For the modeling of 2D-FTS of semiconductor nanostructures, we use a microscopic theory that includes biexcitonic many-body correlations in the coherent $\chi^{(3)}$ limit.[3–5,13,14] In order to keep the numerical complexity manageable, we evaluate this theory for a one-dimensional tight-binding model. This model has been used successfully to obtain results for pump-probe spectra, FWM, and CES signals that are in good qualitative agreement with experiments performed on quantum wells (see Refs. 5 and 20, and references therein). Incorporating the typical selection rules for the excitation of heavy- and light-hole excitonic resonances in III-V semiconductor quantum wells, i.e., two optically uncoupled three-level systems with circularly polarized transitions,[5,20] allows us to model the dependence of 2D-FTS on the polarization directions of the excitation pulses, which is strongly influenced by biexcitonic many-body correlations.[25–27]

The microscopic semiconductor Bloch equations for the interband coherence p and the correlated part of the two-exciton amplitude $\bar{B}$ for coupled heavy- and light-hole excitations can be found in Refs. 5, 20, and 25. In the following, the heavy- and light-hole excitonic resonances are denoted by h and l, respectively. Their homogeneous linewidths are modeled by a phenomenological broadening of $\gamma^{hom}=\hbar/T_2^i$, with $i=h,l$. As we are mainly interested in the action of the homogeneous and inhomogeneous broadening on the spectral features, we assume for simplicity that the magnitudes of the dipole matrix elements and the dephasing times of the h- and l-exciton resonances are equal and that the pulse overlap with these resonances is identical, i.e., the center frequencies of the pulses are in between the resonances. Such an idealized situation is not necessary, but it is chosen to most clearly highlight our approach.

The equations of motion determining the nonlinear optical polarization P are solved numerically, yielding $P(t,\tau,T)$ as a function of time t and time separation τ between the first two pulses (a, b for rephasing mode or b, a for nonrephasing mode). The delay between the second and third pulses, T, is not varied and is fixed to zero here, i.e., second and third pulses arrive at the same time. The nonlinear time-domain polarization is Fourier transformed with respect to t and τ, yielding $P(\omega_t,\omega_\tau,T)$ which, in optically thin structures, is related to the electric field of the signal by $E(\omega_t,\omega_\tau,T) \propto iP(\omega_t,\omega_\tau,T)$. Besides the amplitude $|E(\omega_t,\omega_\tau,T)|$, also the real part $\Re[E(\omega_t,\omega_\tau,T)]$, the imaginary part $\Im[E(\omega_t,\omega_\tau,T)]$, and the phase of the field can be displayed in the two-dimensional frequency space spanned by ω_τ and ω_t. By definition, ω_t is positive, which leads to negative ω_τ in the rephasing case. In these spectra, many signatures depend sensitively on the strengths and ratio of the dipole matrix elements, the dephasing times, and the central frequency of the excitation pulses.[25,27]

Here, we only consider cocircularly, $\sigma^+\sigma^+\sigma^+$, polarized excitation pulses and the same model parameters as used in Fig. 1. If Coulomb correlations are neglected, i.e., on the Hartree-Fock level, this setup generates uncoupled h- and l-exciton transitions. These resonances are, however, coupled by many-body Coulomb correlations, e.g., biexcitons.[5,20,37] In the following, we focus on $\Im[E(\omega_t,\omega_\tau,T)]$ and compare the nonrephasing and rephasing modes (see Fig. 2). Both these modes yield h- and l-excitonic peaks on the diagonal. The line shapes of the signatures on the diagonal of imaginary 2D-FTS show a dispersive character that allows us to suggest a method for the determination of the degree of homogeneous and inhomogeneous broadening. In addition, two off-diagonal features are visible in Fig. 2, which for this polarization scenario are solely due to the aforementioned Coulomb-correlation-induced coupling.[27]

Figure 2 presents homogeneously [Figs. 2(a) and 2(c)] and inhomogeneously [Figs. 2(b) and 2(d)] broadened imaginary 2D-FTS for both modes. Clearly, the nonrephasing (upper panels of Fig. 2) and the rephasing (lower panels of Fig. 2) spectra differ in orientation of the peaks. In the rephasing case, we see the nodes between positive and negative contributions are oriented parallel to the diagonal. In the nonrephasing case, however, the nodes are oriented perpendicular to the diagonal. This constitutes a fundamental difference

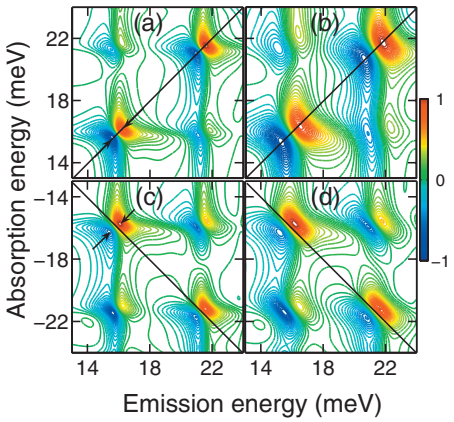

FIG. 2. (Color) Normalized imaginary-part spectra for $\sigma^+\sigma^+\sigma^+$ excitation. For nonrephasing (rephasing) mode, (a) [(c)] homogeneously and (b) [(d)] inhomogeneously broadened spectra are shown. In (b) and (d), the spectra have been broadened by a Gaussian of width $\gamma^{inhom}=0.6$ meV. Dipole matrix elements are taken to be identical, $T_2^{h,l}=1.3$ ps and $T=0$. The arrows in (a) and (c) indicate $\Delta\Omega^{hom}$ of the h exciton. All energies are measured relative to the band gap, which corresponds to 25 meV in our calculations.

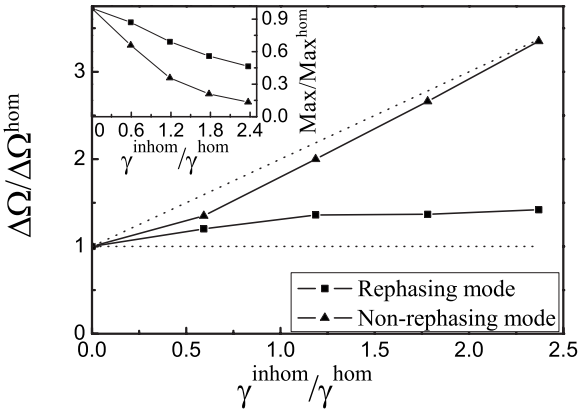

FIG. 3. Ratio $\Delta\Omega/\Delta\Omega^{hom}$ for the h peak as function of $\gamma^{inhom}/\gamma^{hom}$ for inhomogeneous broadenings of $\gamma^{inhom}=0.$, 0.3, 0.6, 0.9, and 1.2 meV and constant homogeneous broadening of $\gamma^{hom}=0.506$ meV. The dotted lines indicate the idealized expectations (see discussion in text). Inset: Dependence of the maxima of amplitude 2D-FTS at the h exciton on $\gamma^{inhom}/\gamma^{hom}$.

in the character of the spectral signatures in the two modes of 2D-FTS. As in, e.g., dispersive off-resonant pump-probe spectra, the energetic separation of positive maxima and negative minima $\Delta\Omega^{hom}$, which for the h-excitonic peak is shown by the arrows in Figs. 2(a) and 2(c), is proportional to the homogeneous linewidth of this particular peak. If only homogeneous broadening is present, the energetic interval $\Delta\Omega^{hom}$ does not depend on the mode of the experiment [cf. Figs. 2(a) and 2(c)] nor does it depend on polarization directions of the incident beams (not shown in figure).

We now phenomenologically incorporate inhomogeneous broadening into our calculations by convoluting the 2D-FTS signal along the diagonal with Gaussian functions of width γ^{inhom}.[5,35] Clearly, this procedure leads to an elongation of the peaks along the diagonal for both the rephasing and the nonrephasing modes. Due to the perpendicular orientation of the dispersive line shape in the nonrephasing and the rephasing cases [see Figs. 2(a) and 2(c)], the inhomogeneous broadening acts differently in the two modes. The main difference is that due to the orientation of the dispersive line shape along the diagonal in the nonrephasing case, the inhomogeneous broadening basically adds to the homogeneous one, while in the rephasing case, due to the perpendicular orientation, the homogeneous and inhomogeneous contributions remain mainly separated.

Also in the presence of inhomogeneous broadening [Figs. 2(b) and 2(d)], we determine the energetic distance between the maxima and minima of the h exciton along the diagonal for nonrephasing spectra and perpendicular to the diagonal for the rephasing spectra, as shown by the arrows in Figs. 2(a) and 2(c); i.e., we use the same definition of $\Delta\Omega$ for the inhomogeneously broadened spectra. To analyze the behavior of $\Delta\Omega$ when inhomogeneous broadening is added, we show in Fig. 3 the ratio $\Delta\Omega/\Delta\Omega^{hom}$ as a function of the input parameters $\gamma^{inhom}/\gamma^{hom}$, i.e., the ratio between inhomogeneous and homogeneous broadening in the model. The dotted lines display the idealized expectations, i.e., $\Delta\Omega/\Delta\Omega^{hom}=1$ for the rephasing case and $\Delta\Omega/\Delta\Omega^{hom}=(\gamma^{inhom}+\gamma^{hom})/\gamma^{hom}$ for nonrephasing mode, respectively. While for the rephasing situation $\Delta\Omega$ stays nearly constant as γ^{inhom} increases, Fig. 3 shows a nearly linear increase for the nonrephasing case. The deviations from the expected dependencies are partly caused by the half-moon shape of the maxima and minima in imaginary 2D-FTS and due to the overlap between the excitonic peaks. In our particular case, we modeled a rather wide quantum well with quite small energetic separation between the h and l excitons, and therefore, the overlap between these resonances rises significantly with increased inhomogeneous broadening. This leads to an increase of the rephasing curve above 1 in Fig. 3, which would be absent for a larger energetic distance between the resonances, e.g., narrower quantum wells.

In the nonrephasing case, the inhomogeneous broadening leads to a partial cancellation of the negative and positive contributions to the imaginary-part spectrum, which does not happen in the rephasing situation. Therefore, we expect a different behavior of the amplitude at the positions of the excitons when including inhomogeneous broadening for the two modes. This is, indeed, the case, as is shown in the inset of Fig. 3, where we have plotted the maximum of the h-exciton amplitude as function of the inhomogeneous broadening. As expected, the decay of the nonrephasing amplitude with inhomogeneous broadening is clearly stronger than that of the rephasing peak; i.e., one can also use the ratio between the rephasing and nonrephasing amplitudes as a measure of the degree of inhomogeneous broadening.

In summary, we have investigated two-dimensional Fourier-transform spectroscopy for a model system which includes heavy- and light-hole excitonic resonances, coherent biexcitonic Coulomb correlations, and inhomogeneous broadening. The emphasis of this work lies on the differ-

ences between the rephasing and the nonrephasing spectra. In particular, the inhomogeneous broadening influences both kinds of spectra in a profoundly different way. This behavior allows us to suggest two-dimensional Fourier-transform spectroscopy as a method for the determination of inhomogeneous broadening in cases where the material system exhibits several, possibly coupled, optical resonances.

This work has been supported by the Optodynamics Center of the Philipps-University Marburg, by the Deutsche Forschungsgemeinschaft (DFG), and by the John-von-Neumann Institute für Computing (NIC), Jülich, Germany. The work at JILA was supported by DOE/BES Grant No. DE-FG02-02ER15346. T.M. thanks the DFG for support through the Heisenberg program (ME 1916/1).

[1] L. Allen and J. H. Eberly, *Optical Resonance and Two-Level Atoms* (Wiley, New York, 1975).
[2] S. Mukamel, *Principles of Nonlinear Optical Spectroscopy* (Oxford, New York, 1995).
[3] H. Haug and S. W. Koch, *Quantum Theory of the Optical and Electronic Properties of Semiconductors*, 4th ed. (World Scientific, Singapore, 2004).
[4] W. Schäfer and M. Wegener, *Semiconductor Optics and Transport Phenomena* (Springer, Berlin, 2002).
[5] T. Meier, P. Thomas, and S. W. Koch, *Coherent Semiconductor Optics—From Basic Concepts to Nanostructure Applications* (Springer, Berlin, 2007).
[6] G. Noll, U. Siegner, S. G. Shevel, and E. O. Göbel, Phys. Rev. Lett. **64**, 792 (1990).
[7] M. Koch, J. Feldmann, G. von Plessen, E. O. Göbel, P. Thomas, and K. Köhler, Phys. Rev. Lett. **69**, 3631 (1992).
[8] V. G. Lyssenko, J. Erland, I. Balslev, K.-H. Pantke, B. S. Razbirin, and J. M. Hvam, Phys. Rev. B **48**, 5720 (1993).
[9] D. S. Chemla and J. Shah, Nature (London) **411**, 549 (2001).
[10] F. Rossi and T. Kuhn, Rev. Mod. Phys. **74**, 895 (2002).
[11] M. Wegener, D. S. Chemla, S. Schmitt-Rink, and W. Schäfer, Phys. Rev. A **42**, 5675 (1990).
[12] M. Lindberg, R. Binder, and S. W. Koch, Phys. Rev. A **45**, 1865 (1992).
[13] V. M. Axt and A. Stahl, Z. Phys. B: Condens. Matter **93**, 195 (1994); **93**, 205 (1994).
[14] M. Lindberg, Y. Z. Hu, R. Binder, and S. W. Koch, Phys. Rev. B **50**, 18060 (1994).
[15] C. Sieh, T. Meier, F. Jahnke, A. Knorr, S. W. Koch, P. Brick, M. Hübner, C. Ell, J. Prineas, G. Khitrova, and H. M. Gibbs, Phys. Rev. Lett. **82**, 3112 (1999).
[16] W. Langbein, T. Meier, S. W. Koch, and J. M. Hvam, J. Opt. Soc. Am. B **18**, 1318 (2001).
[17] E. Finger, S. P. Kraft, M. Hofmann, T. Meier, S. W. Koch, W. Stolz, and W. W. Rühle, Phys. Status Solidi B **234**, 424 (2002).
[18] F. Jahnke, M. Koch, T. Meier, J. Feldmann, W. Schäfer, P. Thomas, S. W. Koch, E. O. Göbel, and H. Nickel, Phys. Rev. B **50**, 8114 (1994).
[19] T. F. Albrecht, K. Bott, T. Meier, A. Schulze, M. Koch, S. T. Cundiff, J. Feldmann, W. Stolz, P. Thomas, S. W. Koch, and E. O. Göbel, Phys. Rev. B **54**, 4436 (1996).
[20] T. Meier and S. W. Koch, in *Semiconductors and Semimetals*, edited by K. T. Tsen (Academic, New York, 2001), Vol. 67, pp. 231–313.
[21] S. Weiser, T. Meier, J. Möbius, A. Euteneuer, E. J. Mayer, W. Stolz, M. Hofmann, W. W. Rühle, P. Thomas, and S. W. Koch, Phys. Rev. B **61**, 13088 (2000).
[22] T. Zhang, C. N. Borca, X. Li, and S. T. Cundiff, Opt. Express **13**, 7432 (2005).
[23] C. N. Borca, T. Zhang, X. Li, and S. T. Cundiff, Chem. Phys. Lett. **416**, 311 (2005).
[24] X. Li, T. Zhang, C. N. Borca, and S. T. Cundiff, Phys. Rev. Lett. **96**, 057406 (2006).
[25] I. Kuznetsova, P. Thomas, T. Meier, T. Zhang, X. Li, R. P. Mirin, and S. T. Cundiff, Solid State Commun. **142**, 154 (2007).
[26] L. Yang, I. V. Schweigert, S. T. Cundiff, and S. Mukamel, Phys. Rev. B **75**, 125302 (2007).
[27] T. Zhang, I. Kuznetsova, T. Meier, X. Li, R. P. Mirin, P. Thomas, and S. T. Cundiff, Proc. Natl. Acad. Sci. U.S.A. **104**, 14227 (2007).
[28] R. R. Ernst, G. Bodenhausen, and A. Wokaun, *Principles of Nuclear Magnetic Resonance in One and Two Dimensions* (Oxford Science, New York, 1987).
[29] O. Golonzka, M. Khalil, N. Demirdöven, and A. Tokmakoff, Phys. Rev. Lett. **86**, 2154 (2001).
[30] M. T. Zanni, N.-H. Ge, Y. S. Kim, and R. M. Hochstrasser, Proc. Natl. Acad. Sci. U.S.A. **98**, 11265 (2001).
[31] S. Mukamel, Annu. Rev. Phys. Chem. **51**, 691 (2000).
[32] J. D. Hybl, A. A. Ferro, and D. M. Jonas, J. Chem. Phys. **115**, 6606 (2001).
[33] T. Brixner, J. Stenger, H. M. Vaswani, M. Cho, R. E. Blankenship, and G. R. Fleming, Nature (London) **434**, 625 (2005).
[34] A. Euteneuer, E. Finger, M. Hofmann, W. Stolz, T. Meier, P. Thomas, S. W. Koch, W. W. Rühle, R. Hey, and K. Ploog, Phys. Rev. Lett. **83**, 2073 (1999).
[35] T. Meier, C. Sieh, E. Finger, W. Stolz, W. W. Rühle, P. Thomas, and S. W. Koch, Phys. Status Solidi B **238**, 537 (2003).
[36] S. T. Cundiff, M. Koch, W. H. Knox, J. Shah, and W. Stolz, Phys. Rev. Lett. **77**, 1107 (1996).
[37] P. Brick, C. Ell, G. Khitrova, H. M. Gibbs, T. Meier, C. Sieh, and S. W. Koch, Phys. Rev. B **64**, 075323 (2001).